[1]UniFi [2] INFN Firenze [3] INAF OAA

SUPERNOVA REMNANTS
AN ODYSSEY IN SPACE AFTER STELLAR DEATH
6 - 11 JUNE 2016, CHANIA, CRETE, GREECE

Newest insights from MHD numerical modeling of Pulsar Wind Nebulae

B. Olmi[1,2,3], L. Del Zanna[1,2,3], E. Amato[3], N. Bucciantini[1,2,3], R. Bandiera[3]

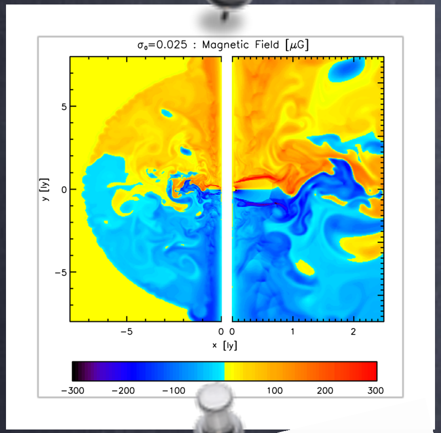
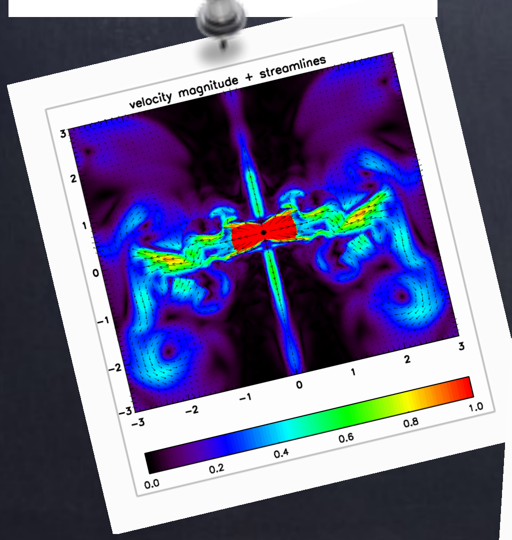

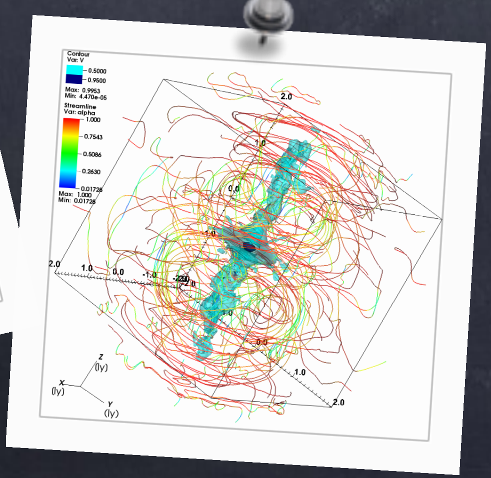
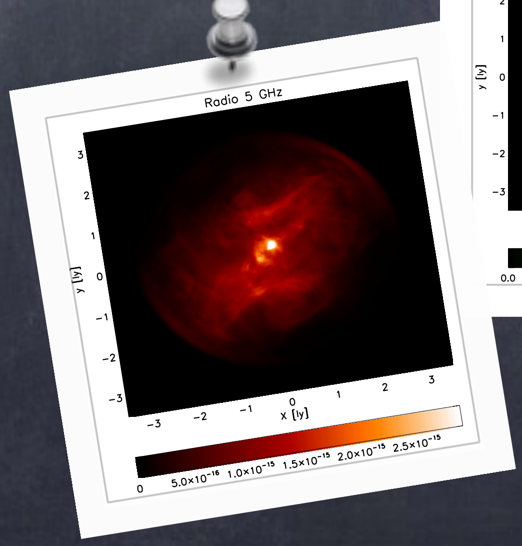

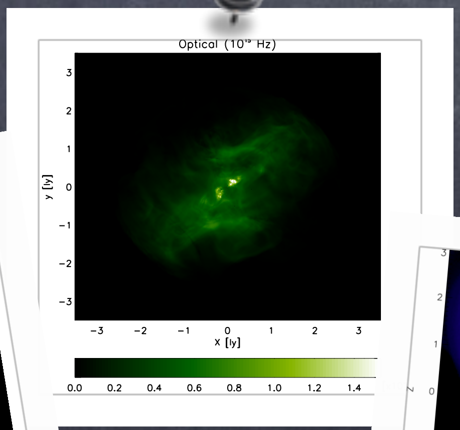
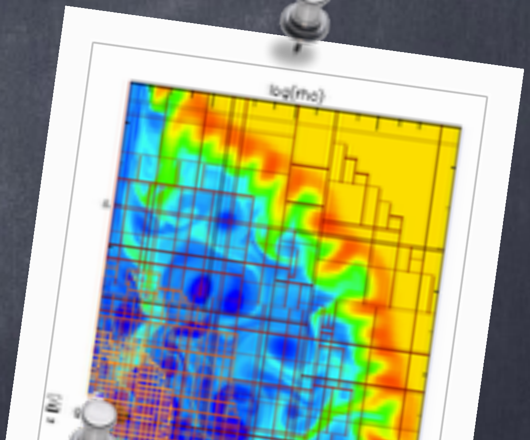
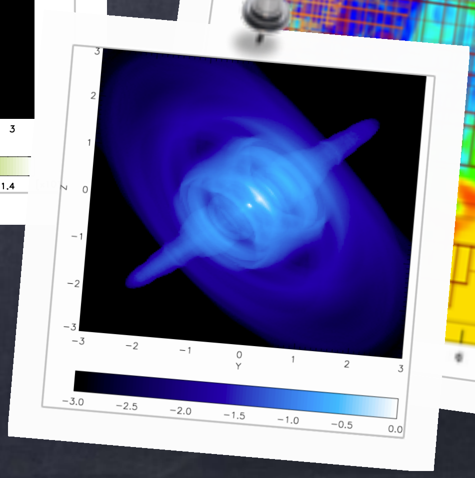

Why we need numerical simulations?

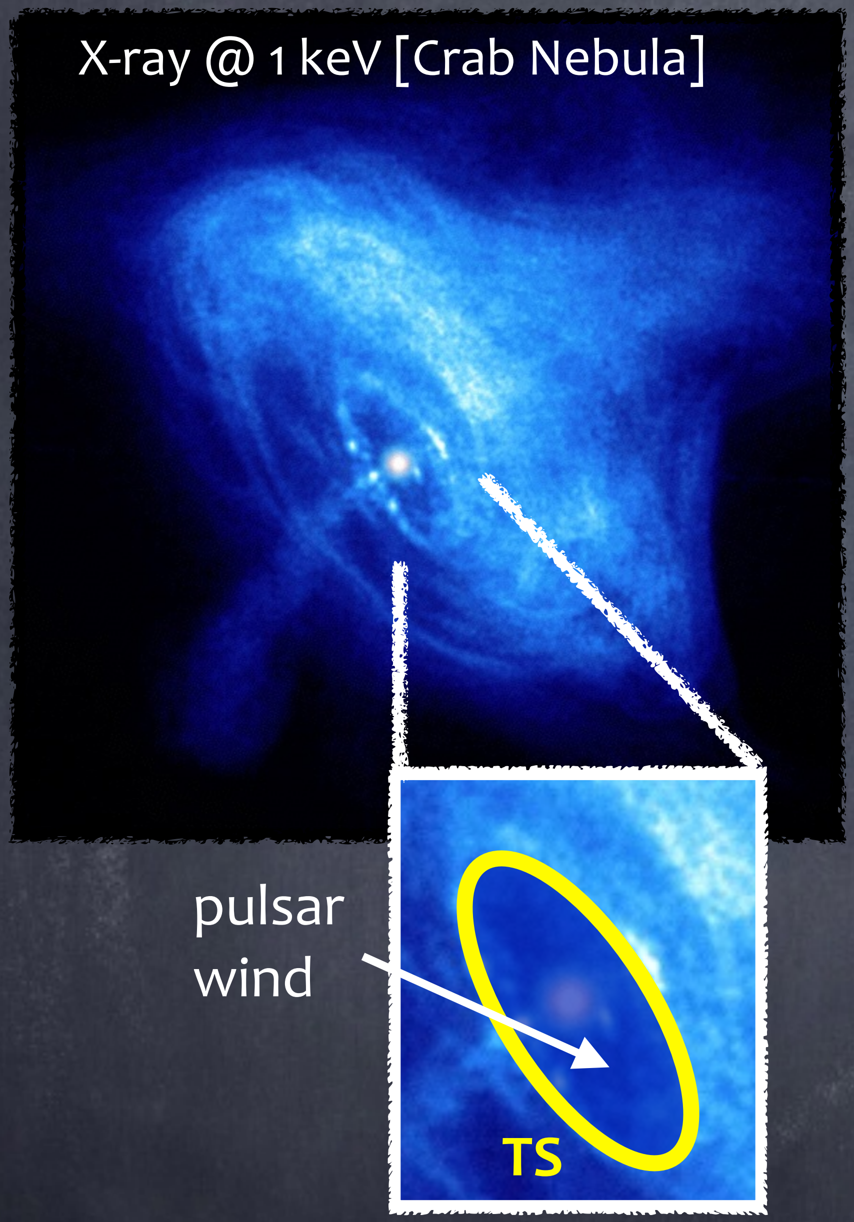

PWNe are powered by the spin-down of young NSs that lose their energy in the form of a relativistic, magnetized and cold wind.

- Wind composition: (e^+ - e^-) pairs + possibly a small amount of hadrons.
- Observational properties: it appears as a sub-luminous area in the center of the nebula. The inner ring is usually associated to the TS shock location.

⬇

No emission = no direct information about the physics of the wind!

The numerical model:
main properties of the pulsar wind

[Michel 1973, Bogovalov 1999, Contopoulos + 1999, Coroniti 1990, Gruzinov 2004, Lyubarsky 2002]

1

Define a PW model

- Anisotropic distribution of the energy flux $F(r,\vartheta)$:

$$F(r,\theta) \propto \frac{\alpha + (1-\alpha)\sin^2\theta}{(2+\alpha)r^2} \rightarrow F(r,\pi/2) \gg F(r,0) \rightarrow \alpha \ll 1$$

anisotropy parameter

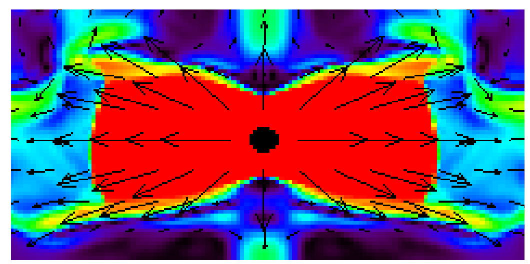

Oblate TS, with $r_{eq} > r_{pol}$

- Striped morphology within an equatorial belt of extension ≃ 2×ζ

$$B(r,\theta) \propto \sqrt{\sigma}\sin\theta\tanh\left[b\left(\frac{\pi}{2}-\theta\right)\right]$$

initial wind magnetization

width of striped zone

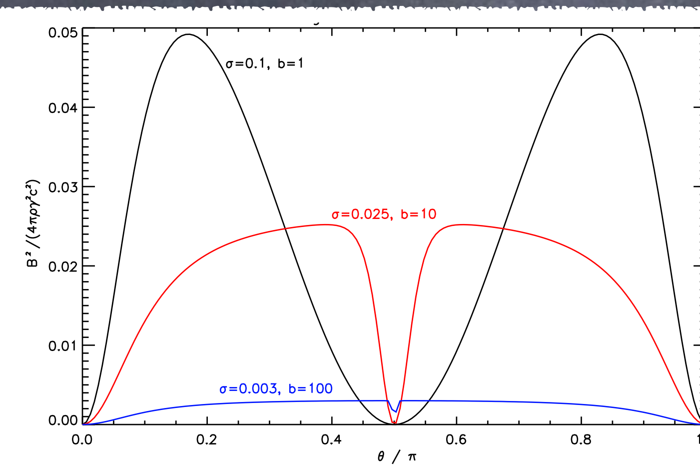

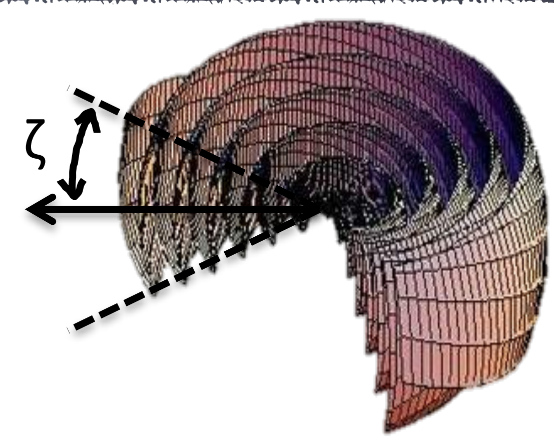

b ≫ 1 ⇒ NO STRIPES

b ~ 1 ⇒ STRIPES (wider for smaller b)

(α, b, σ) →FREE PARAMETERS of the numerical model

[Formulas from: Del Zanna + 2006, Olmi + 2014]

The numerical model

(α, b, σ)

1 Define a PW model

2 Simulate the system up to $t=t_{CRAB} \simeq 1000$ yr

obtain synthetic maps

3 Compare with observed properties

find the best fit (α, b, σ)

From 2D simulations:
$\alpha = 0.1$
$b = 10$
$\sigma = 0.025$

Crab in Radio [NRAO]
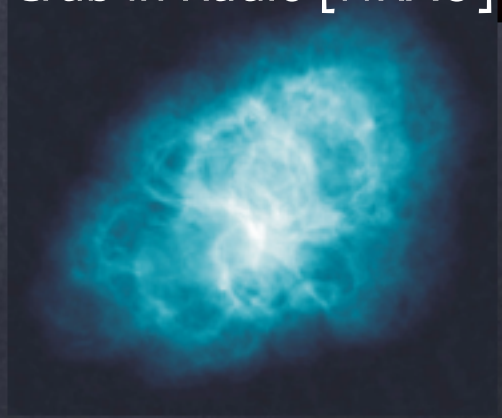

Particle acceleration in PWNe

PWNe are powerful accelerators: evidence for PeV electrons

BUT acceleration takes place in a very hostile environment: the relativistic and magnetized shock of the PW!

Proposed mechanisms at Crab TS:

[Amato 2014]

Fermi I → particles gain energy in multiple shock crossings

- [x] Correct slope for optical/X-ray spectrum $N(E) \propto E^{-p},\ p = 2$
- [ ] Requires low magnetization to be efficient at relativistic shocks ($\sigma<0.001$)

[Spitkovsky 2008, Sironi & Spitkovsky 2011]

Driven Magnetic Reconnection → particles accelerated in strong reconnecting regions

- [x] Correct slope for radio spectrum $N(E) \propto E^{-p},\ 1 \lesssim p \lesssim 1.5$
- [x] Requires high magnetization
- [ ] Requires large pulsar pair multiplicity ($\kappa \gtrsim 10^8$)

Maybe can work only in small sectors

[Lyubarsky 2003, Lyubarsky & Liverts 2008, Sironi & Spitkovsky 2011]

Crab wisps as probes of the particle acceleration mechanism

(1) From MHD models:

Wisps are proven to simply trace the local properties of the underlying flow (B field + Doppler boosting). Wisps are reproduced, almost identical, under different hypotheses for radio particles origins.

[Olmi et al 2014]

Radio wisps maps @ 5 GHz

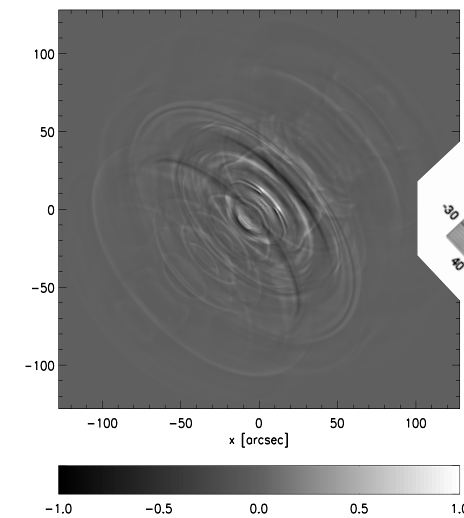

Radio particles as part of the pulsar outflow (injected at TS)

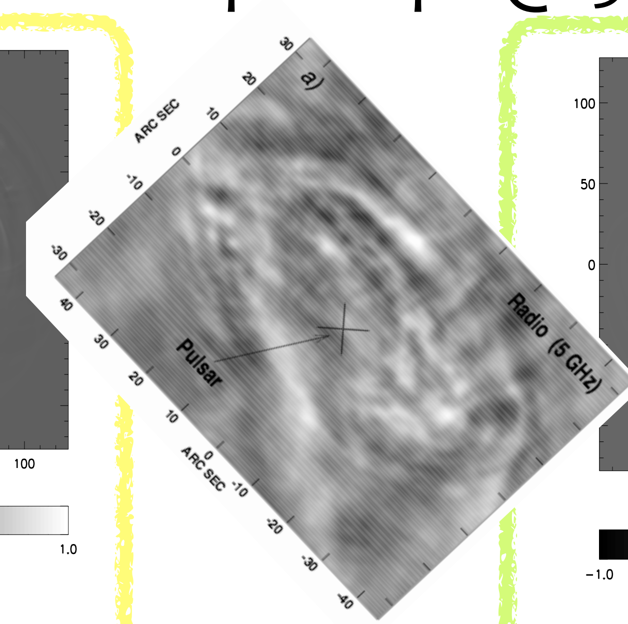

[Bietenholz + 04]

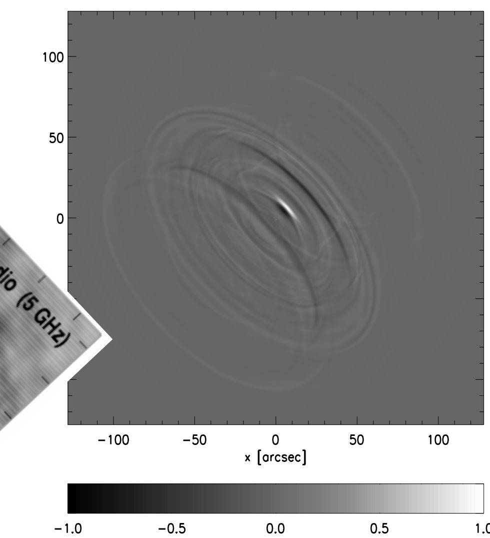

Radio particles are produced elsewhere (isotropic distribution)

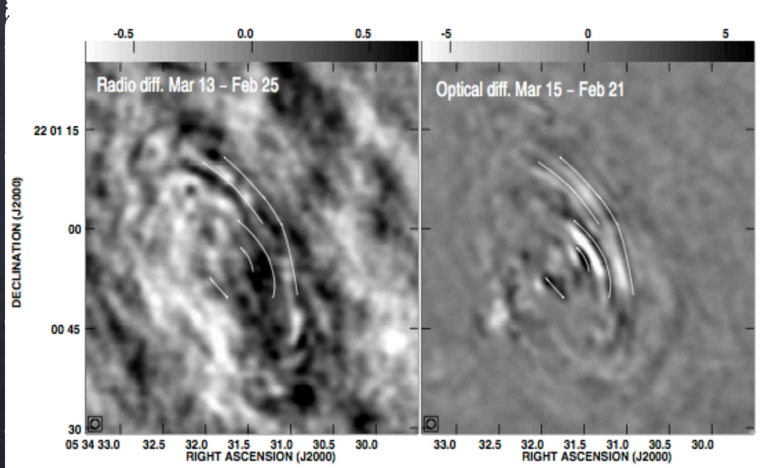

[Bietenholz et al 2004]

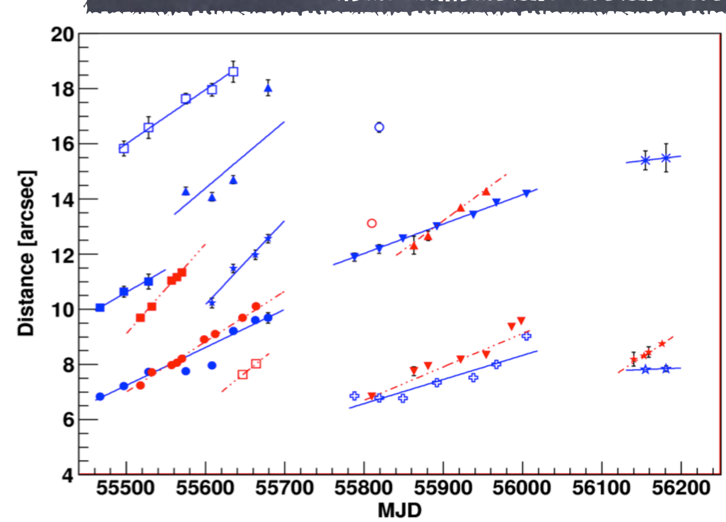

[Schweizer et al 2013]

(2) From observations:

Wisps are seen at multi-λ with non-coincident locations and different outward velocities ($0.1c \lesssim v \lesssim 0.4c$)

Crab wisps as probes of the particle acceleration mechanism

Radio wisp maps @ 5 GHz

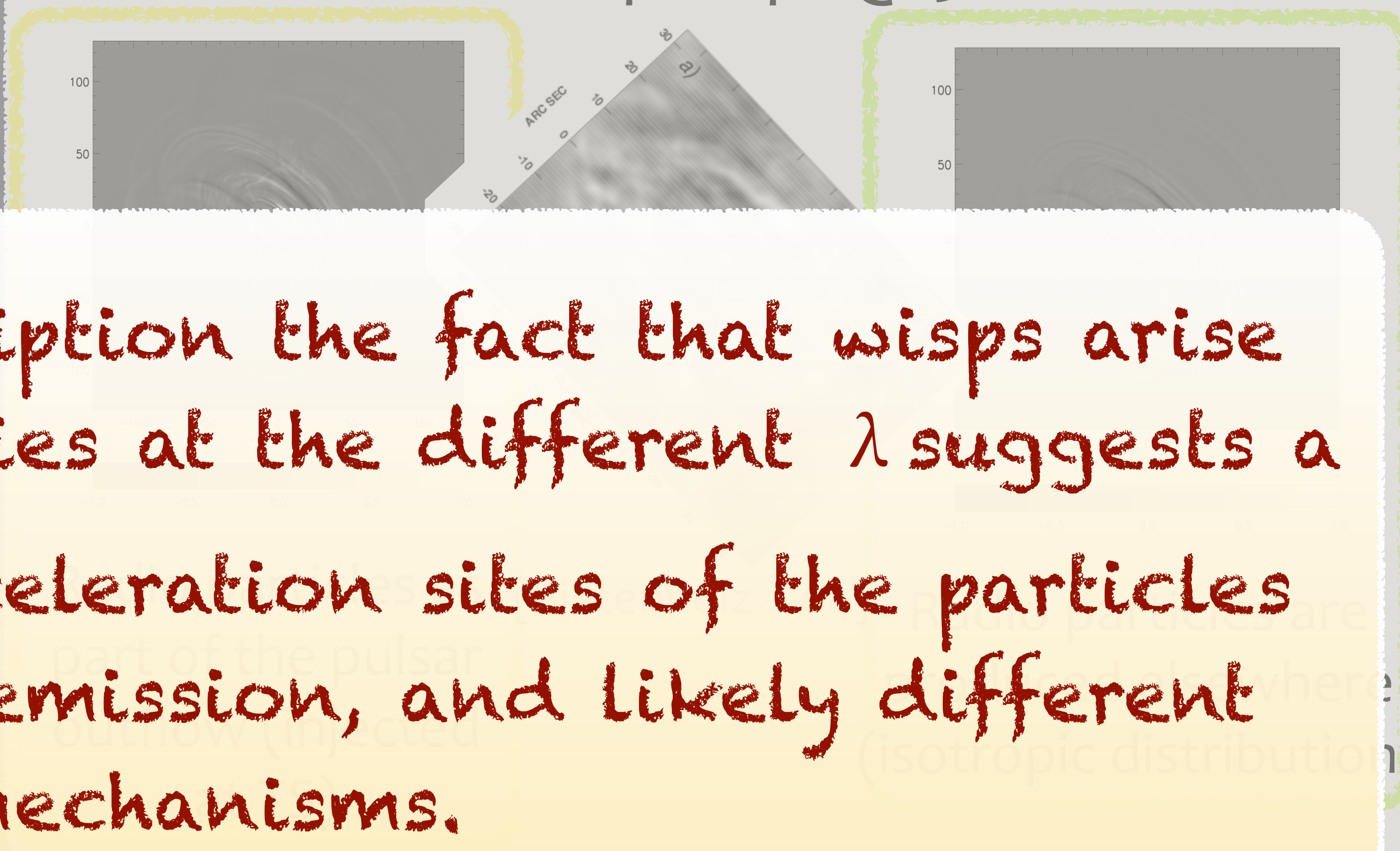

Wisps are proven to simply trace the local properties of the

Within an MHD description the fact that wisps arise with different properties at the different λ suggests a difference in the acceleration sites of the particles responsible for the emission, and likely different mechanisms.

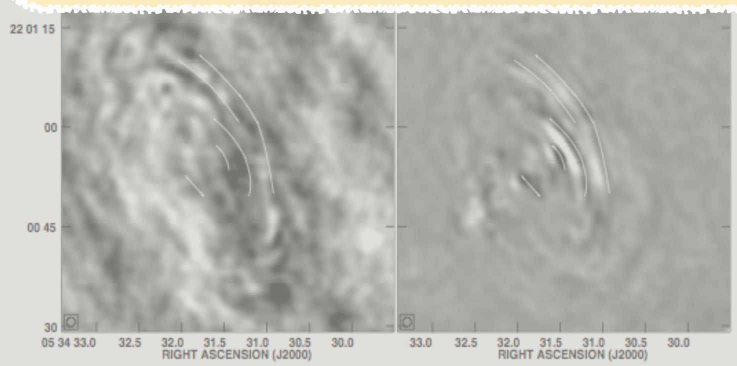

[Bietenholz et al 2004]

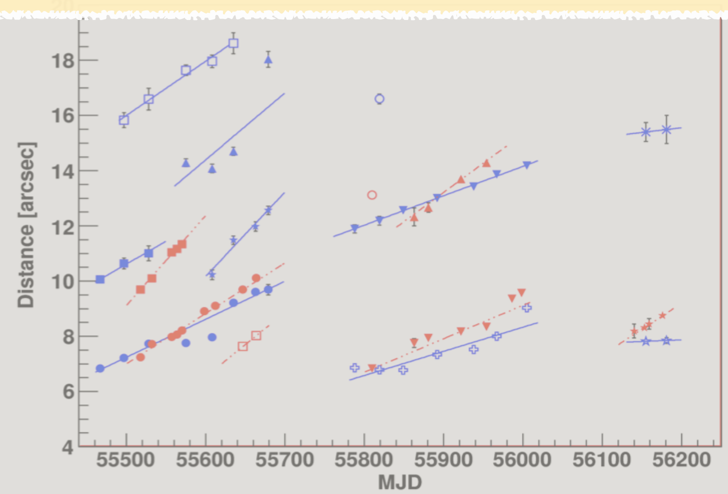

[Schweizer et al 2013]

Wisp are seen at multi-λ with non-coincident locations and different outward velocities ($0.1c \lesssim v \lesssim 0.4c$)

Multi wavelengths wisp analysis

[Olmi et al 2015]

We investigate the acceleration mechanism by injecting the emitting particles within different angular sectors at the PW shock:

(1) Uniform injection → $\theta \in [0°, 180°]$

(2) Injection in a wide equatorial zone → $\theta \in [20°, 160°]$ or in the opposite narrow polar one → $\theta \in [0°, 20°] \cup [160°, 180°]$

(3) Injection in a narrow equatorial zone → $\theta \in [70°, 110°]$ or in the opposite wide polar one → $\theta \in [0°, 70°] \cup [110°, 180°]$

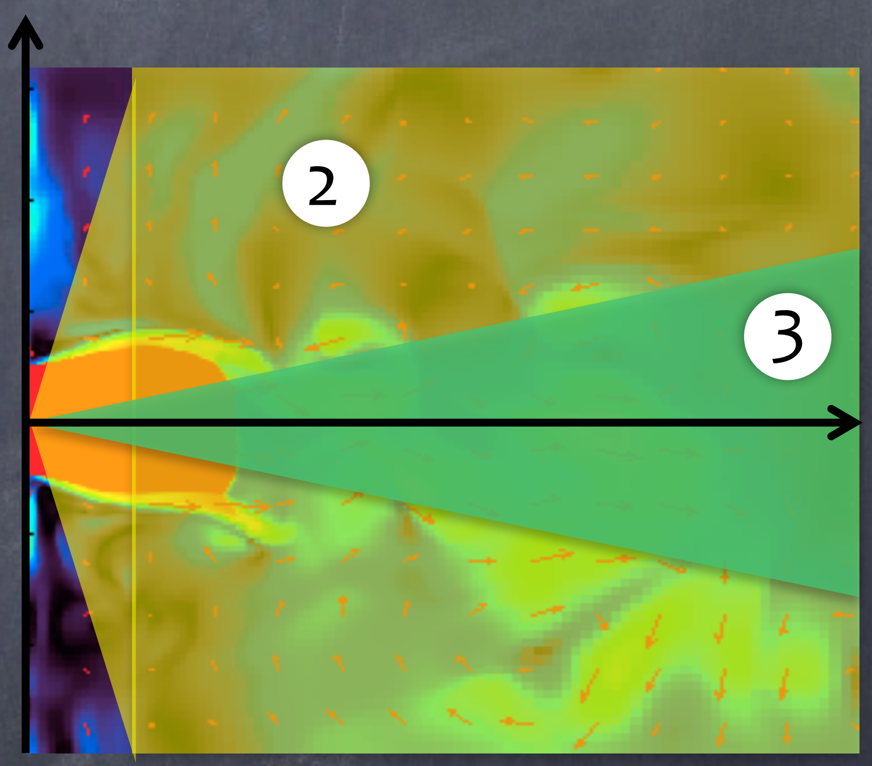

Multi wavelengths wisp analysis

[Olmi et al 2015]

Synchrotron emission properties are obtained considering two distinct particle families (radio and X-ray) and optical emission is obtained as a mixed contribution:

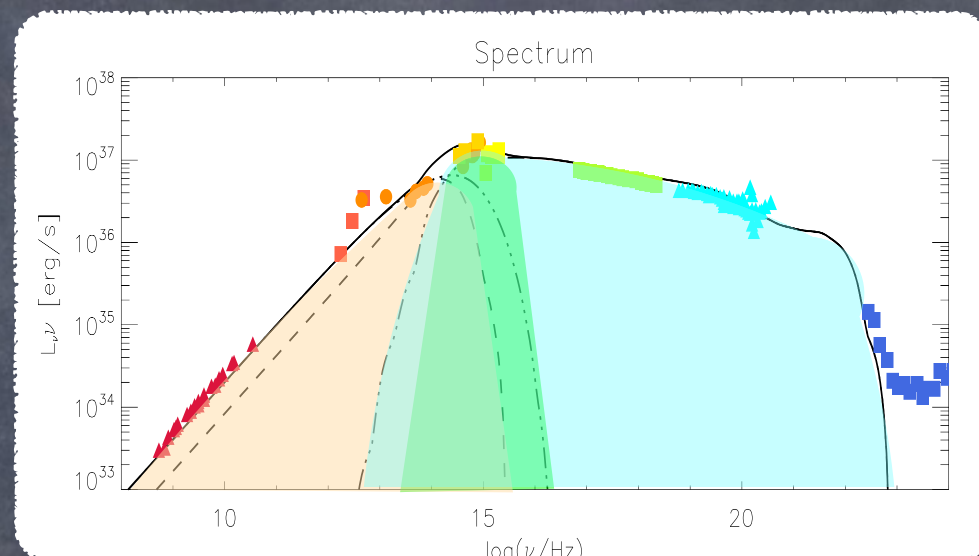

* Radio particles

* Optical particles

* X-ray particles

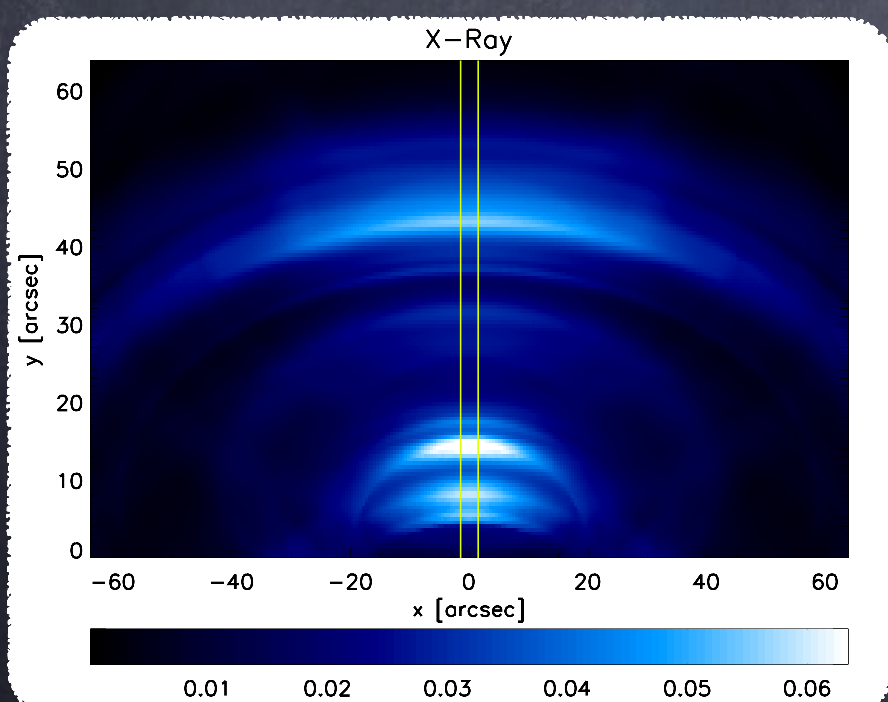

Data sample: monthly outputs over 10 yr around $t=t_{Crab}$.

Wisps profiles extracted from a 3” slice in the upper hemisphere of intensity maps following the analysis in Schweizer et al 2013.

Results: (1) Uniform injection

[Olmi et al 2015]

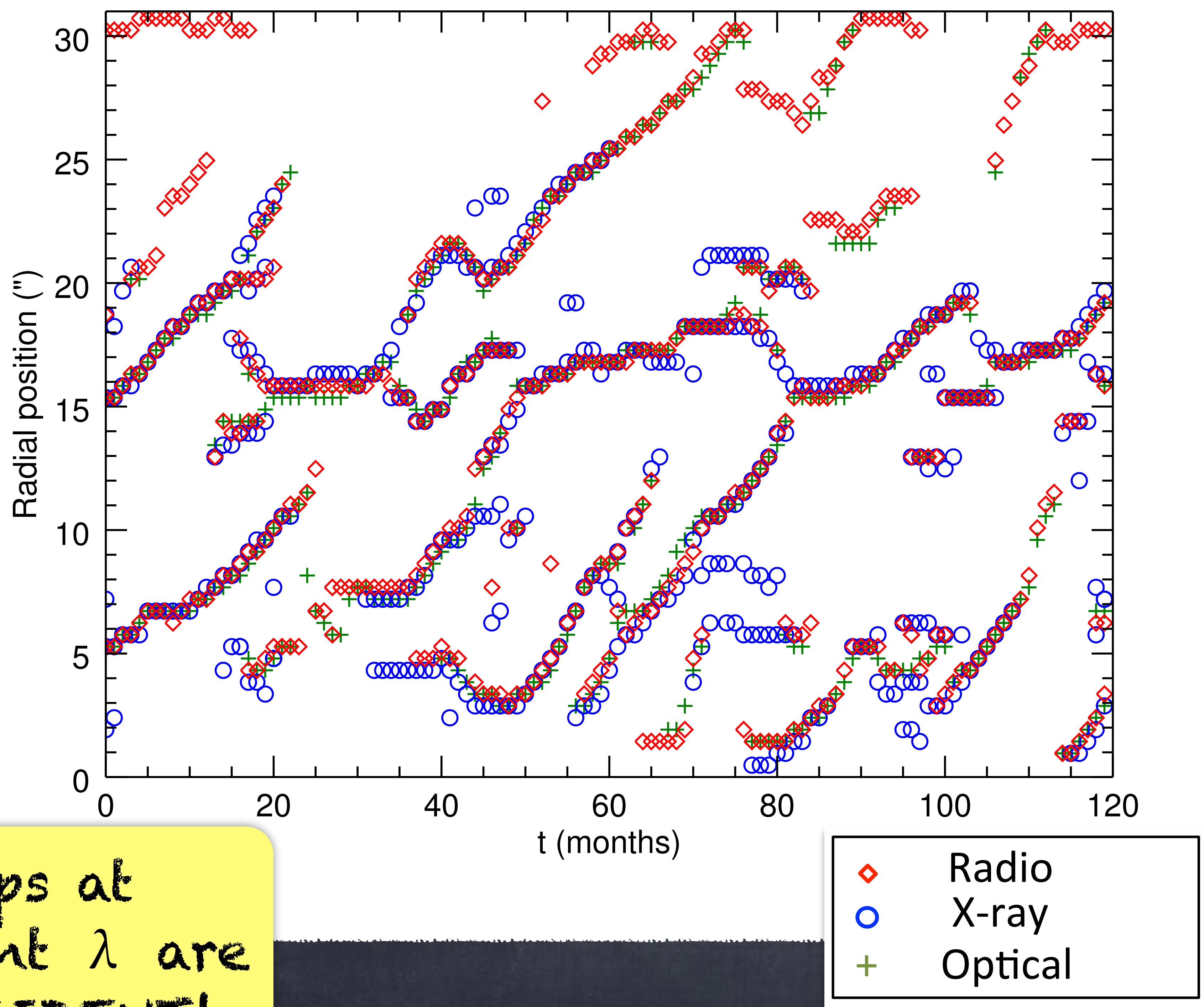

Wisps at different λ are COINCIDENT!

Results: (2) Wide eq + narrow pole

[Olmi et al 2015]

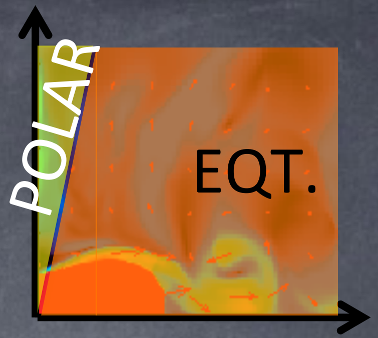

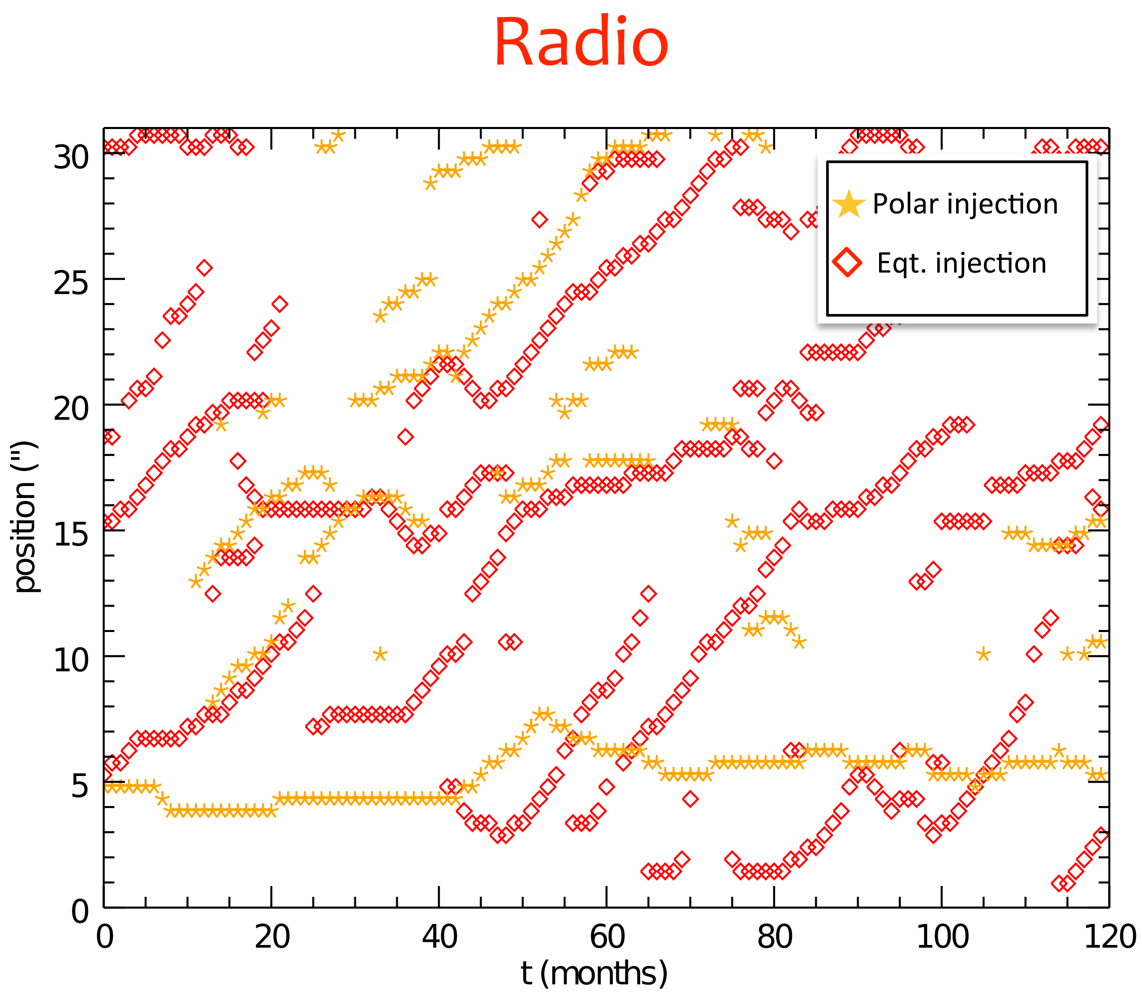

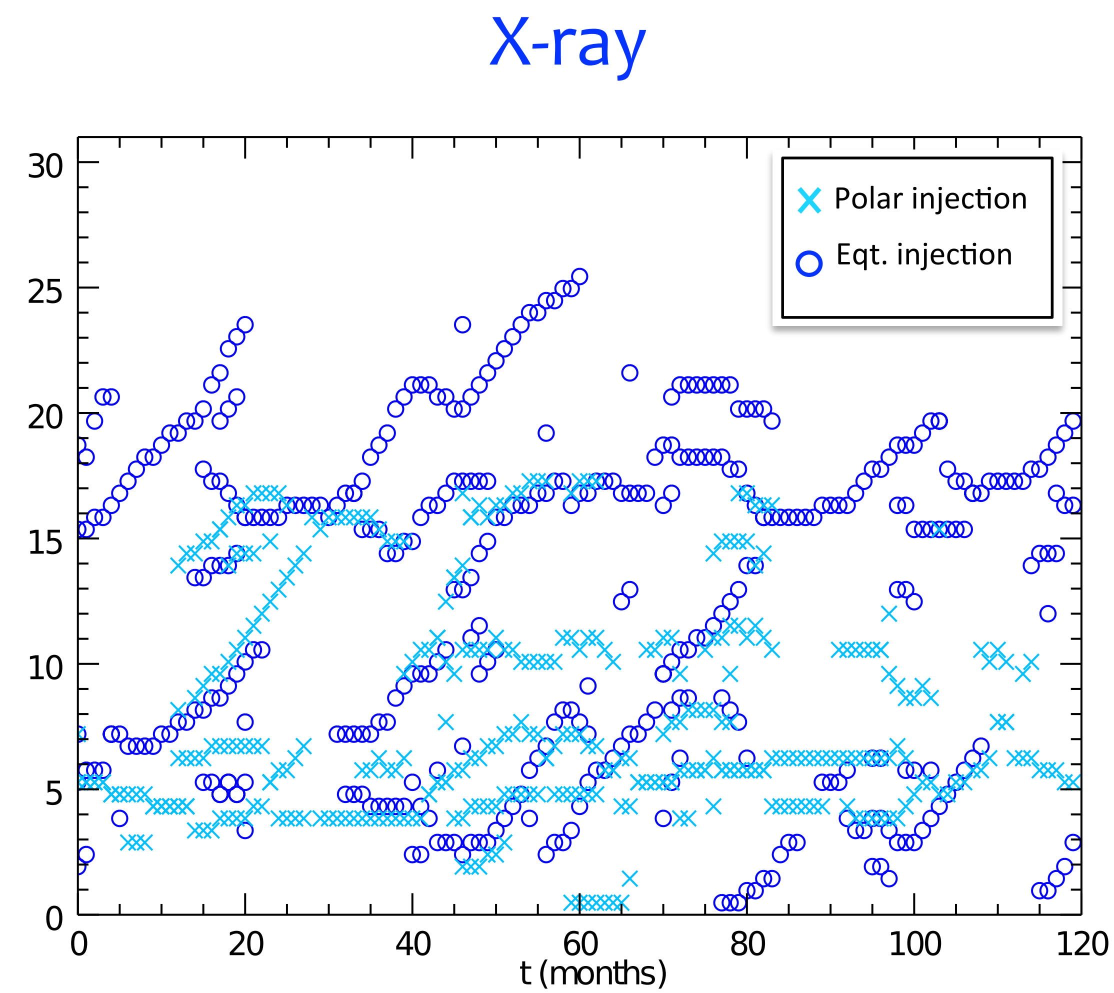

X and ✳ → basically NO wisps

○ and ◇ → identical to uniform injection

No way to reproduce observations injecting particles in opposite sectors

Results: (3) Narrow eq + wide pole

[Olmi et al 2015]

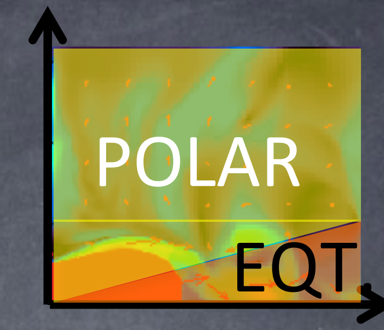

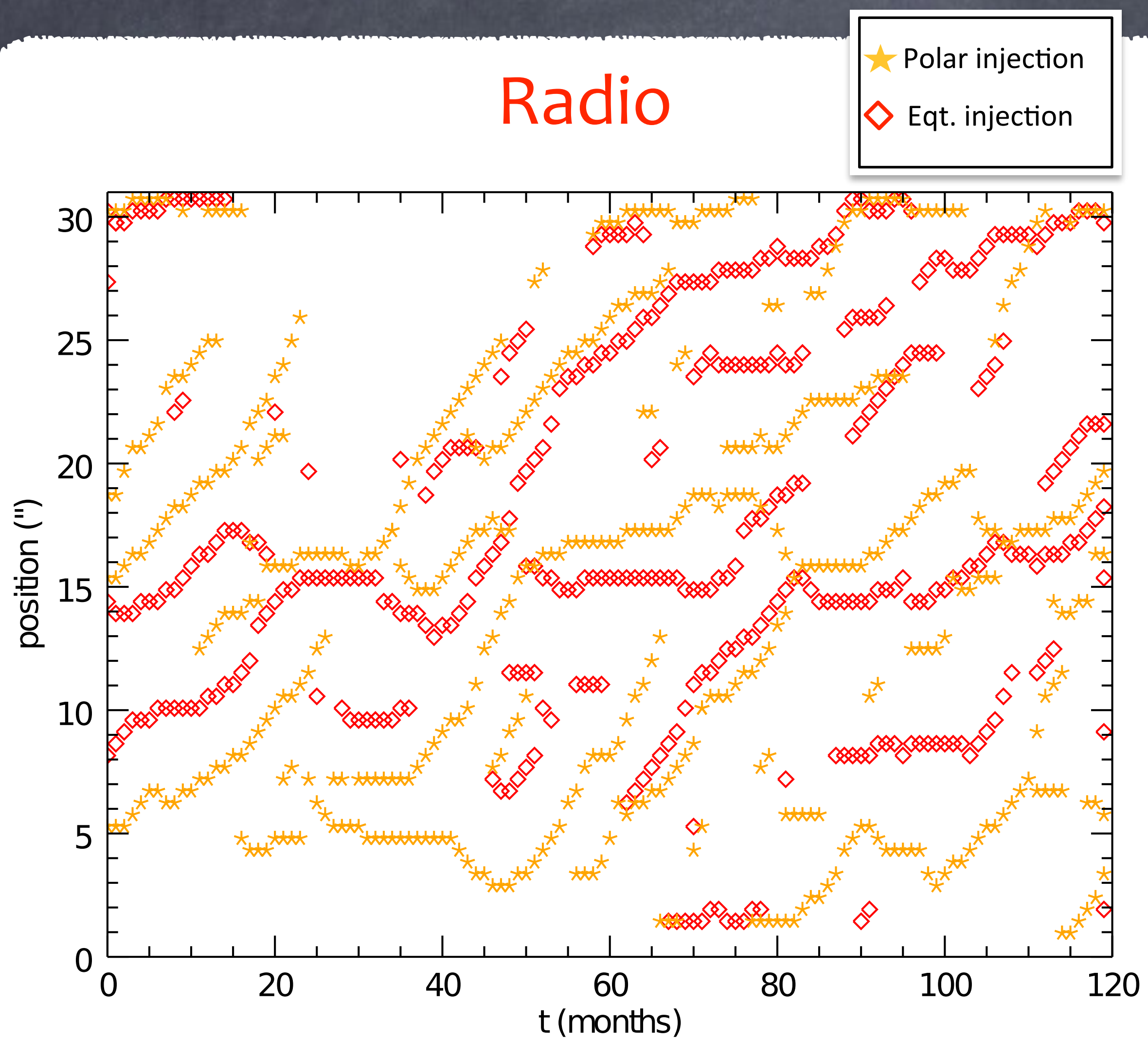

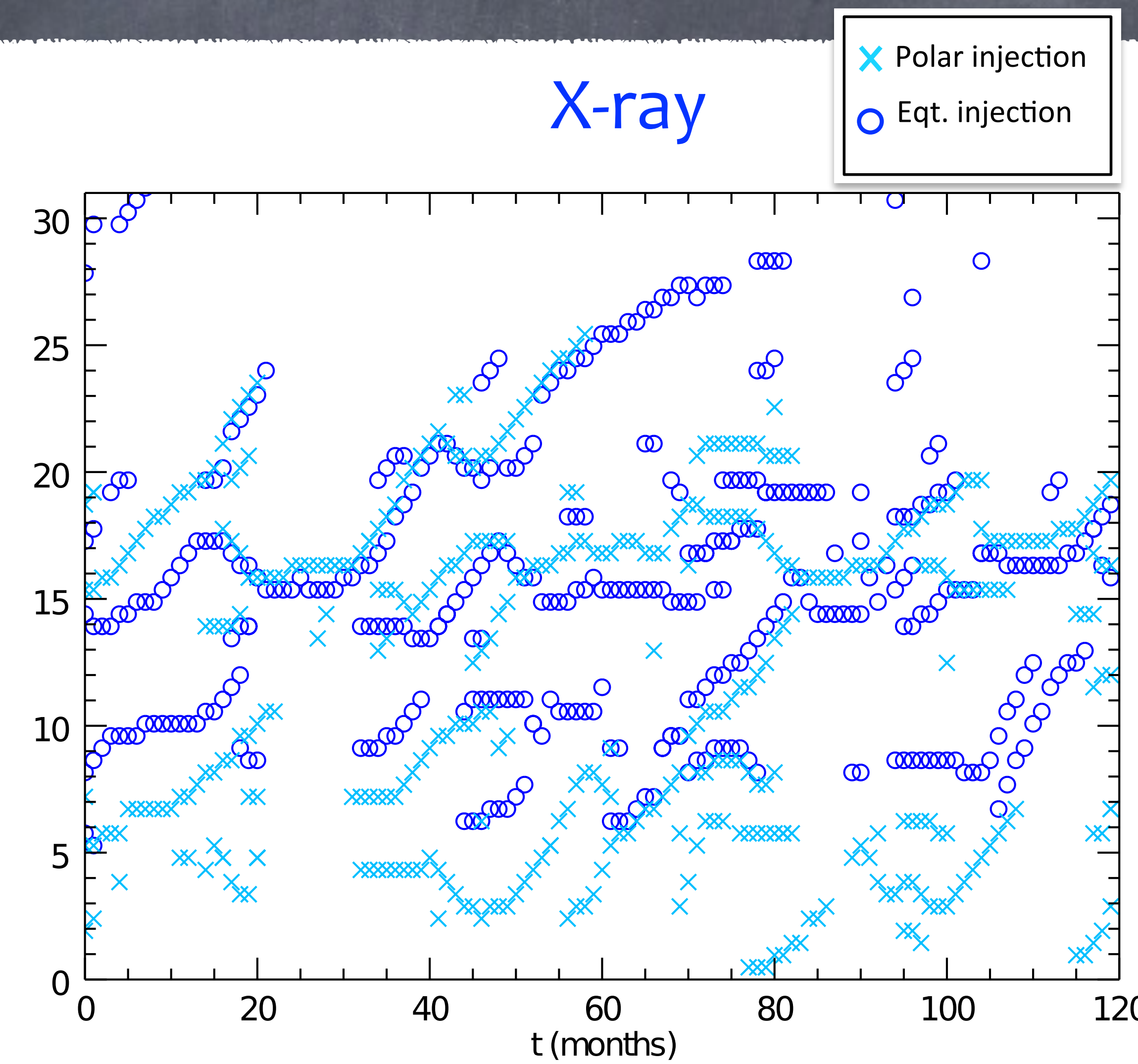

Wisps appear in both cases!

Results: (3) Narrow eq + wide pole

[Olmi et al 2015]

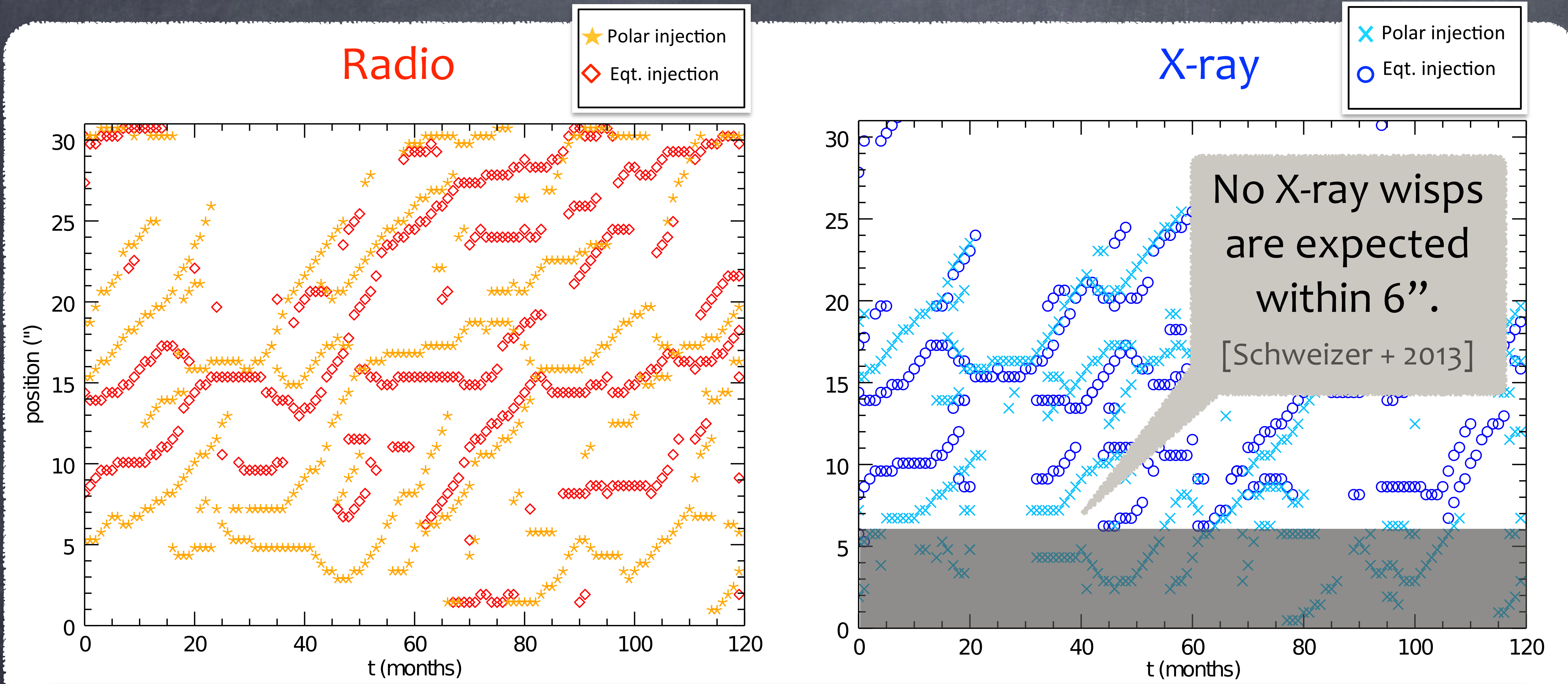

X-ray particles must be injected in a narrow eq. zone (θ∈[70°,110°]).
Radio emission is difficult to constrain: to have radio wisps not coincident with X-ray ones, radio particles must be injected in the polar sector or in a wider equatorial one.

Deprojected wisps outward velocities:
$0.08c \leq v \leq 0.38c$

$0.1c \lesssim v \lesssim 0.4c$ from observations

Conclusions and perspectives

Facts:

- ✓ Wisps can be used to test different injection scenario for the emitting particles.
- ✓ Different acceleration mechanisms require different physical conditions, not satisfied at the same locations around TS.
- ✓ To have non coincident wisps at the different λ the corresponding emitting particles must be injected and accelerated in different sectors.

Results:

The multi-λ analysis of wisps properties shows that the most promising scenario for particle acceleration at the Crab TS is:

- X-ray particles injected in a narrow equatorial sector (~ striped zone of wind) → compatible with Fermi I acceleration
- Radio particles injected in the opposite polar sector (or in a wider equatorial one) → where conditions for driven magnetic reconnection might be locally satisfied

Conclusions and perspectives

What's next?

2D axisymmetric models have proven to be extremely efficient at accounting for many of the observed properties of PWNe, especially concerning the high energy emission.

Some problems still remain without answer:

- sigma paradox
- integrated spectrum
- low-energy emission and large scale emission
- magnetic field structure and mean value

→ Solution (?): 3D models!

First 3D simulation by Porth et al 2013 + 2014 solve some open questions, but it only reproduced ~ 70 yr of the Crab age —> too short for complete emission modeling.

Preliminary results from 3D long term simulation of the Crab Nebula by Olmi, Del Zanna, Mignone:

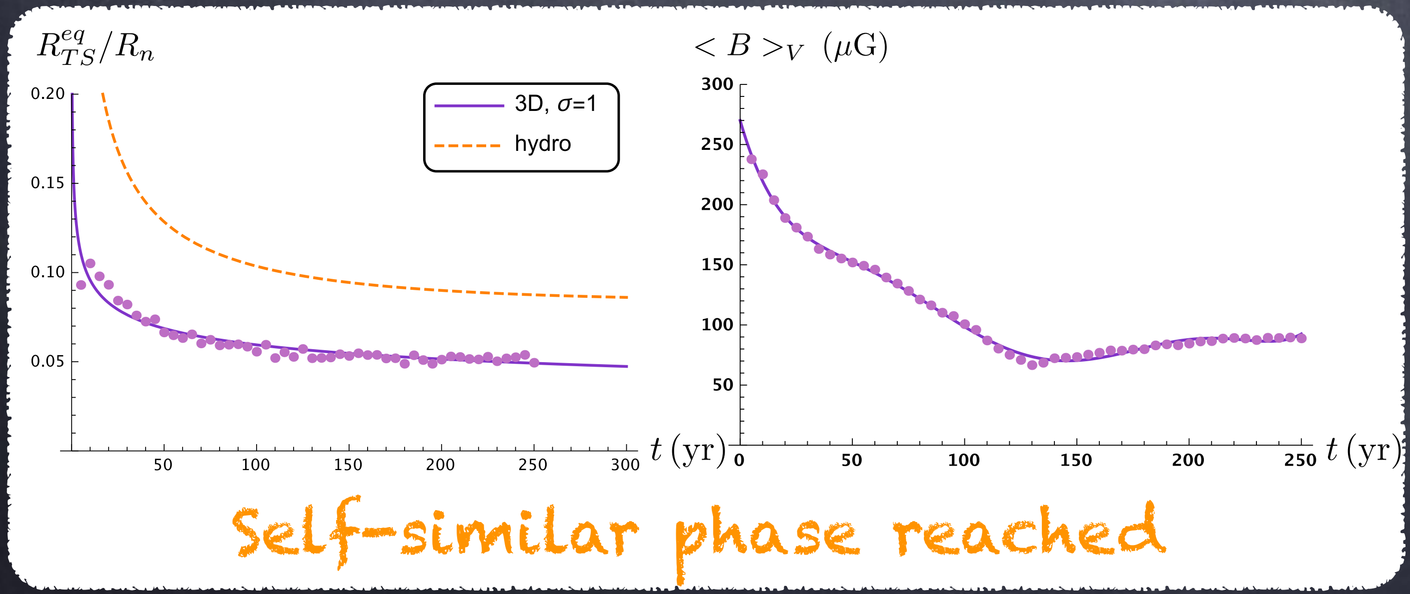

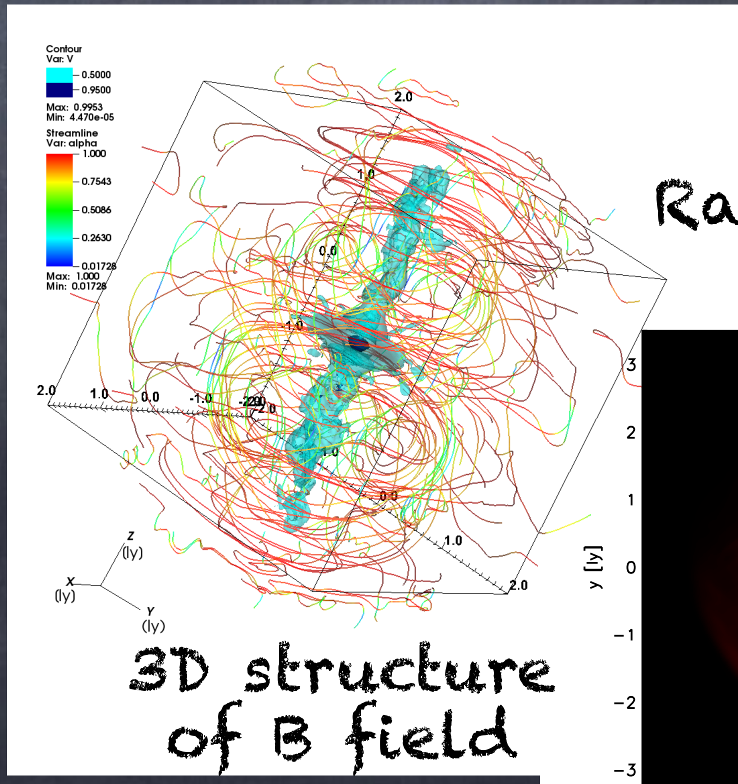

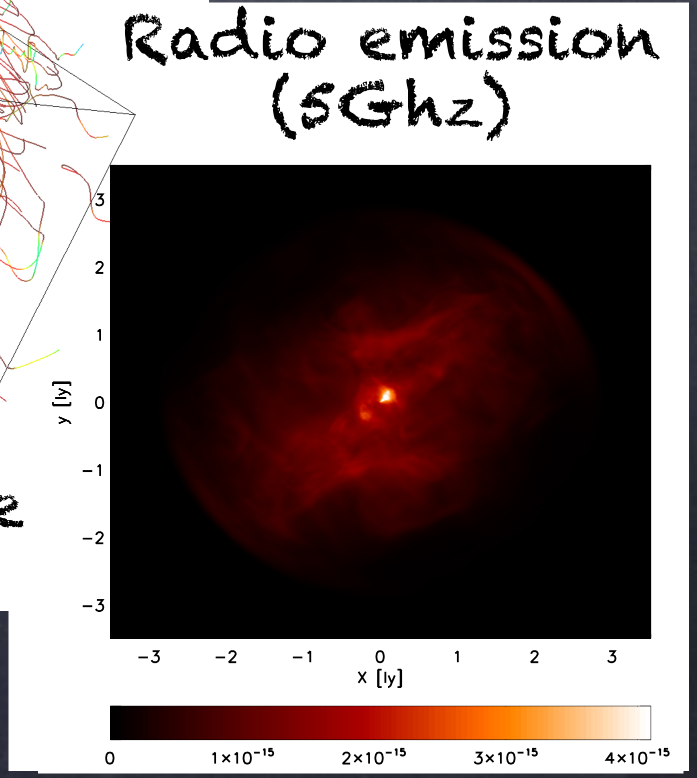

Thank you for your attention!

Back up slides

Radio and X-ray families

[Olmi et al 2015]

Synchrotron emission properties are obtained considering two distinct particle families:

- Radio particles:

$$f_{0\mathrm{R}}(\epsilon_0) \propto \begin{cases} 0 & \text{if} \quad \epsilon_0 < \epsilon_{\mathrm{minR}} \\ \epsilon_0^{-p_\mathrm{R}} \exp(-\epsilon_0/\epsilon^*_\mathrm{R}) & \text{if} \quad \epsilon_0 > \epsilon_{\mathrm{minR}} \end{cases}$$

- X-ray particles:

$$f_{0\mathrm{X}}(\epsilon_0) \propto \begin{cases} 0 & \text{if} \quad \epsilon_0 < \epsilon_{\mathrm{minX}} \\ \epsilon_0^{-p_\mathrm{X}} \exp(-\epsilon_0/\epsilon^*_\mathrm{X}) & \text{if} \quad \epsilon_0 > \epsilon_{\mathrm{minX}} \end{cases}$$

Limits and spectral indices are chosen in order to fit the integrate spectrum

Optical particles are then obtained as a mixed contribution of radio and X-ray families

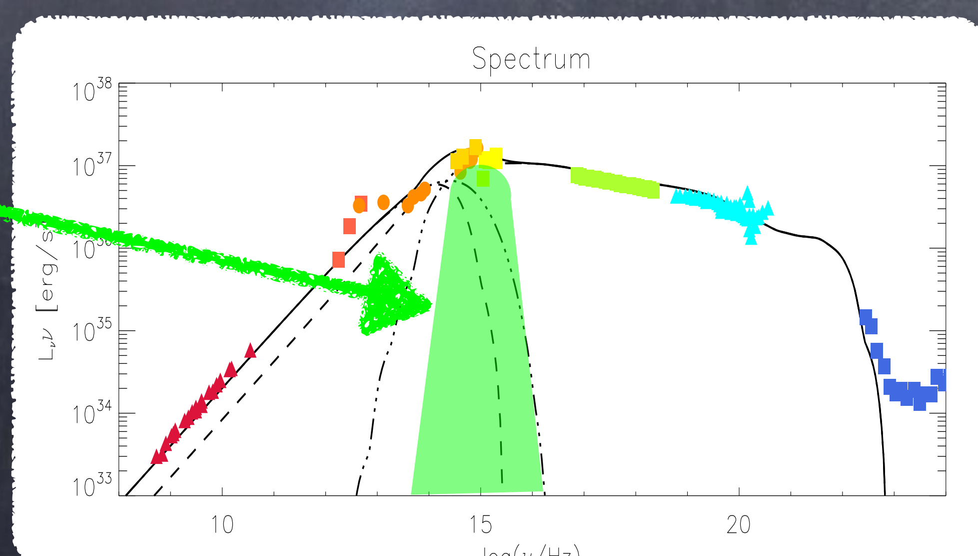

Radio	X-ray
p	p
ε	ε
ε	ε

Velocity of wisps (case (3))

[Olmi et al 2015]

Outward velocities computed from most prominent wisps:

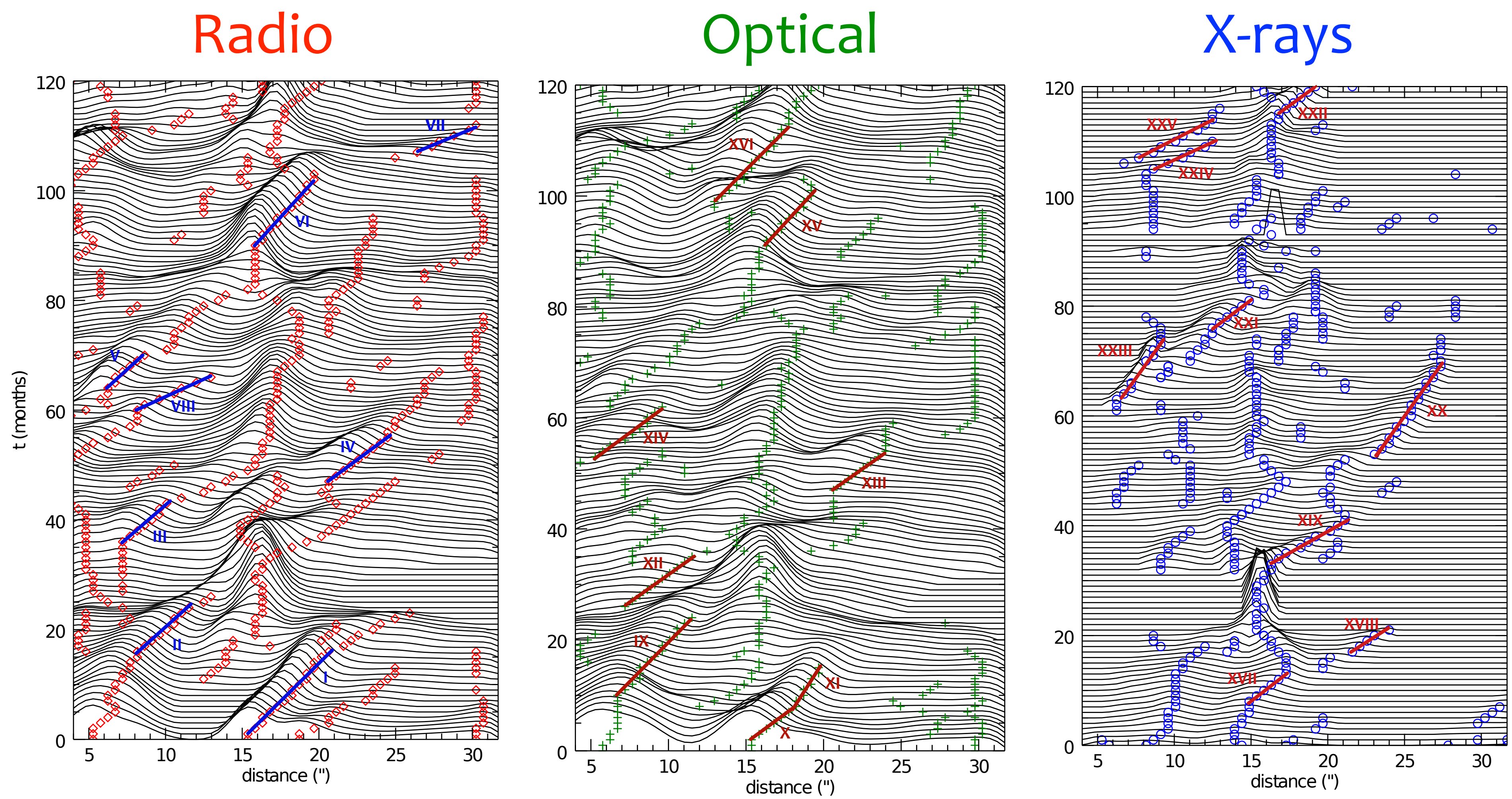

Radio				Optical				X-ray			
Wisp #	v_{app} (arcsec d^{-1})	v_{app}/c	v/c	Wisp #	v_{app} (arcsec d^{-1})	v_{app}/c	v/c	Wisp #	v_{app} (arcsec d^{-1})	v_{app}/c	v/c
I	0.012	0.14	0.16	IX	0.011	0.13	0.15	XVII	0.016	0.18	0.21
II	0.014	0.16	0.18	X	0.016	0.18	0.21	XVIII	0.018	0.21	0.24
III	0.016	0.18	0.21	XI	0.007	0.08	0.09	XIX	0.020	0.23	0.27
IV	0.015	0.17	0.20	XII	0.016	0.18	0.21	XX	0.009	0.10	0.12
V	0.013	0.15	0.17	XIII	0.015	0.17	0.20	XXI	0.013	0.15	0.17
VI	0.010	0.11	0.13	XIV	0.016	0.18	0.21	XXII	0.018	0.21	0.24
VII	0.027	0.31	0.36	XV	0.011	0.13	0.15	XXIII	0.009	0.10	0.12
VIII	0.029	0.33	0.38	XVI	0.011	0.13	0.15	XXIV	0.026	0.30	0.35
								XXV	0.023	0.26	0.30

Optical wisps (case (3)):

[Olmi et al 2015]

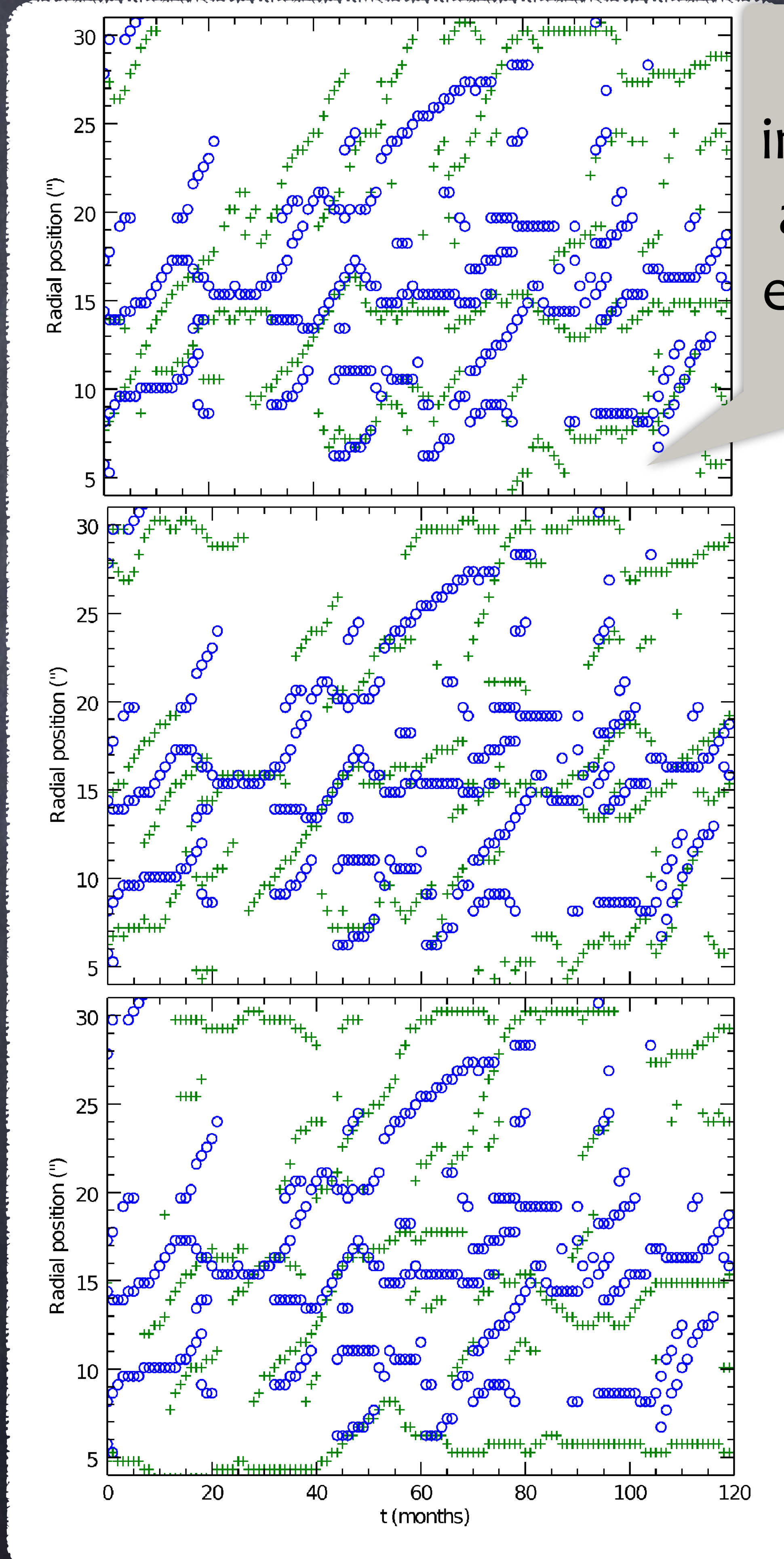

X-ray injected in a narrow equatorial sector

Radio injected under different hypotheses